Imaging the membrane protein bacteriorhodopsin with the atomic force microscope

Hans-Jürgen Butt, Kenneth H. Downing,* and Paul K. Hansma
Department of Physics, University of California, Santa Barbara, California 93106, and *Donner Laboratory, Lawrence Berkeley Laboratory, Berkeley, California 94720 USA

ABSTRACT The membrane protein bacteriorhodopsin was imaged in buffer solution at room temperature with the atomic force microscope. Three different substrates were used: mica, silanized glass and lipid bilayers. Single bacteriorhodopsin molecules could be imaged in purple membranes adsorbed to mica. A depression was observed between the bacteriorhodopsin molecules. The two dimensional Fourier transform showed the hexagonal lattice with a lattice constant of 6.21 ± 0.20 nm which is in agreement with results of electron diffraction experiments. Spots at a resolution of ~1.1 nm could be resolved.

A protein, cationic ferritin, could be imaged bound to the purple membranes on glass which was silanized with aminopropyltriethoxysilane. This opens the possibility of studying receptor/ligand binding under native conditions.

In addition, purple membranes bound to a lipid bilayer were imaged. These images may help in interpreting results of functional studies done with purple membranes adsorbed to black lipid membranes.

INTRODUCTION

The atomic force microscope (AFM), invented by Binnig, Quate, and Gerber in 1986 (1), is a new scanning probe microscope for investigating surfaces (2). In the AFM, the sample is placed on a xyz translator and raster scanned below a stylus which has been mounted on a cantilever (Fig. 1). Forces exerted by surface features cause the stylus to defect the cantilever. The deflection of the cantilever is measured by detecting the angular deflection of a laser beam reflected off the back of the cantilever. Surface topography is determined by using a feedback loop. The feedback loop keeps the cantilever deflection constant by moving the sample up and down as the stylus traces over the contours of the surface. An image is obtained by plotting the vertical motion of the xyz translator as a function of lateral position.

AFMs have been able to image different materials with atomic resolution (3, 4). In biology the AFM has been used to image amino acid crystals (5), proteins (6), DNA (7), organic monolayers or bilayers (7, 8), and whole cells (9). Even a process, the polymerization of fibrinogin, has been imaged (6). The AFM is a promising tool for studying membrane proteins because it can image individual molecules in buffer and at room temperature (6).

Purple membranes are particularly suitable for applying the AFM to membrane proteins. The purple membrane is a specialized part of the cell membrane of *Halobacterium halobium.* It consists of a two-dimensional crystalline array of a single protein, called bacteriorhodopsin. Bacteriorhodopsin uses energy of light absorbed by its chromophore retinal to pump protons across the cell membrane. The structure of bacteriorhodopsin has been studied by different techniques. X-Ray diffraction experiments showed that bacteriorhodopsin is packed in a hexagonal lattice with P3 symmetry (10, 11). Using low-dose, cryoelectron microscopy to obtain electron diffraction patterns and high-resolution images, Henderson and co-workers have determined the three-dimensional structure of bacteriorhodopsin to a resolution of 0.35 nm parallel and 0.7 nm perpendicular to the membrane (12–14). Based on these data they derived an atomic model. They showed that the protein contains seven α-helical segments which extend roughly perpendicular to the plane of the membrane for most of its width. Neutron diffraction analysis from specifically deuterated specimens determined the positions of the chromophore (15, 16) and of several helices (17–19).

The AFM has already been used to image dried purple membranes (9, 20, 21). In this work we have developed three model systems to image bacteriorhodopsin in buffer solution. Imaging in buffer has the advantage, that the specimen can be maintained in its native state and that the forces applied to the sample can be reduced (22). First, purple membranes were adsorbed to mica. Individual bacteriorhodopsin molecules could be identified. The two-dimensional Fourier transform showed spots out to the fifth order corresponding to a resolution of ~1.1 nm. Guckenberger et al. (23) obtained high resolution images

Dr. Butt's present address is Max-Planck-Institut für Biophysik, Kennedyallee 70, D-6000 Frankfurt 70 FRG.

0006-3495/90/12/1473/08 $2.00

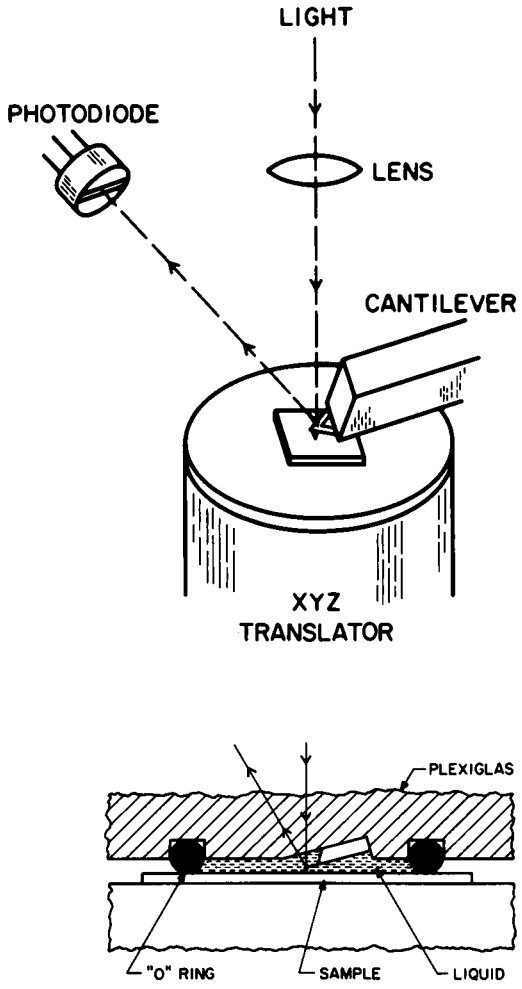

FIGURE 1 Schematic diagram of our AFM. Laser light is focused on a cantilever which reflects it towards two segments of a photodiode. These two segments sense the deflection of the reflected beam and, thus, the deflection of the cantilever. In operation a feedback loop controls the position of the cantilever and, hence, the force on the sample. This is accomplished by moving the sample up and down as the sample is scanned underneath it.

of the HPI layer with the scanning tunneling microscope in air. However, to our knowledge these are the first high-resolution scanning probe microscope images of a membrane protein in buffer solution.

In addition, purple membranes were bound to glass silanized with aminopropyltriethoxysilane. Then the binding of cationized ferritin to these purple membranes could be imaged. Third, purple membranes were adsorbed to a lipid bilayer. This system resembles that used in functional experiments where purple membranes were adsorbed to black lipid membranes (24, 25 and references therein).

MATERIALS AND METHODS

The atomic force microscope

The sample is glued to a steel disc and placed on an electrically grounded magnetic disc on top of an xyz translator (Fig. 1). The xyz translator had a scan range of 20 μm. The scanning was activated by applying voltages across the piezo translator, controlled by modified software and hardware from Nanoscope II (Digital Instruments, Goleta, CA). To obtain one image the scanning time ranged from 4 to 80 s for scan widths of 50 nm to 20 μm, respectively.

The xyz translator scans the sample under a stylus mounted to a cantilever. The stylus interacts with the surface and the cantilever is deflected. Sorts of cantilevers used are given in Table 1. Cantilevers of different lengths were used. Short cantilevers have a high sensitivity but apply a higher force to the sample (26). In addition, cantilever type A and B had diamonds as styluses glued to the microfabricated Si_3N_4 lever, whereas the stylus of cantilever type C was microfabricated of Si_3N_4 too (Park Scientific, Mountain View, CA).

To measure the deflection of the cantilever, our AFM uses the light beam of a laser diode which is focused onto the end of the cantilever. The reflection from the back of the cantilever is picked up by two segments of a photodiode (model Spot-4D; United Detector Technology, Hawthorne, CA) and the difference in intensity measured by the two segments is used as a signal (27–29). Using this signal, a feedback loop controls the z motion of the xyz translator. The cantilever is kept at a constant deflection and, hence, the force applied by the stylus is kept constant. The variable voltage applied to the z segment is used as the image contrast. Each image stored consisted of 400 × 400 points. Our microscope was equipped with a sealed liquid cell on top of the scanner which enclosed the sample and the cantilever.

Sample preparation

Purple membranes were prepared from *Halobacterium halobium* strain JW3 according to Oesterhelt and Stoeckenius 1974 (30). Before each experiment the purple membrane solution was sonicated for 20 s in a bath sonicator.

Purple membranes on mica: 50 μl of purple membrane solution at a concentration of 40 μg/ml were pipetted onto freshly cleaved green muscovite mica which was glued to a steel disc. After 10 min the sample was placed in the microscope and the rest of the volume was filled with pure buffer.

Purple membranes on silanized glass: microscope cover glasses with a diameter of 12 mm were cleaned with detergent, water, ethanol and hexane. Then they were placed in a glass desiccator together with 2 ml of 3-aminopropyltriethoxysilane in an open Petri dish. The desiccator was closed and evacuated. After 2 h the glass discs were put in an oven for 2 h at 130°C (31) to bind the aminopropyltriethoxysilane covalently to the

TABLE 1

Type	Length	Stylus	Spring constant	Force
	μm		N/m	nN
A	100	Diamond	0.33	0.7
B	200	Diamond	0.18	0.5
C	200	Microfabr.	0.12	0.3

Cantilevers used in this study. The spring constants were calculated by A. Weisenhorn, personal communication. The force is the force applied to the sample.

glass surface. 50 μl of purple membrane at a concentration of 40 μg/ml were pipetted on the glass. 10 min later we began imaging after the rest of the volume was filled up with pure buffer solution. Cationized ferritin (ferritin from horse spleen coupled with *N,N*-dimethyl-1,3-propanediamine) was purchased from Sigma Chemical Co., St. Louis, MO.

Purple membranes on a lipid bilayer: lipid bilayers were formed on mica with arachidic acid as the bottom layer and DL-α-dimyristoylphosphatidyl-choline (DMPC) as the top layer according to Weisenhorn et al., 1990 (7). Both lipids were used as purchased without further purification. Monolayer films of arachidic acid were spread from a chloroform solution (1 mg/ml) at the air/water interface of a homemade Langmuire trough. After the chloroform was allowed to evaporate for several minutes, the film was compressed to a final pressure of 30 mN/m. Then a green muscovite mica piece which was submerged in the trough prior to film formation was slowly pulled out at an angle of roughly 40° to the water surface. In this way a monolayer of arachidic acid was formed on the mica surface. Then the trough was cleaned and a DMPC monolayer was formed from a chloroform solution (1 mg/ml). The film was transferred to the arachidic acid monolayer by vertically dipping the mica piece through the air water interface. Distilled water was used for the second layer whereas the bottom monolayer was formed in 0.5 mM $CdCl_2$. The samples were transferred in distilled water to the microscope. We started to image 10 min after adding purple membranes suspended in distilled water at a concentration of 80 μg/ml.

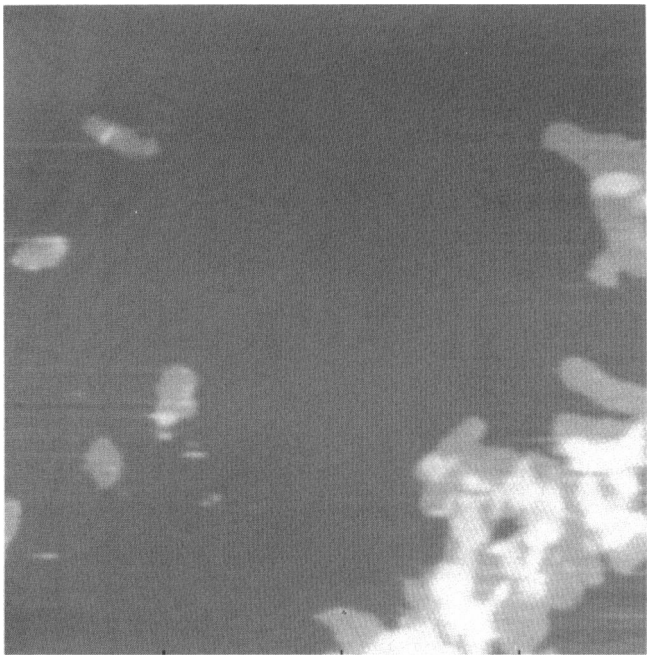

FIGURE 2 Purple membranes adsorbed to mica imaged with the AFM. Light parts are high, dark parts are low. The purple membranes were imaged in 2 mM $CaCl_2$, 80 mM KCl, 10 mM KH_2PO_4, and pH 4.0 with a type B cantilever (see Table 1). The image size is 8.2 × 8.2 μm.

RESULTS AND DISCUSSION

Adsorbance of purple membranes to mica, silanized glass, and lipid bilayers

Purple membranes on mica: it is known that negatively charged molecules poorly adsorb to mica (32). As purple membranes are negatively charged at neutral pH the first step was to find conditions where the membrane sheets adsorb to mica. Therefore, the calcium concentration had to be carefully adjusted. At calcium concentrations <1 mM no adsorption was observed whereas at calcium concentrations of 5 mM and above the purple membranes formed stacks. To get single membrane sheets adsorbed to mica we chose a buffer composed of 2 mM $CaCl_2$, 50–100 mM KCl or NaCl, and a pH ranging from pH 4.0 to 6.5. A typical image of purple membranes adsorbed to mica is shown in Fig. 2. It can be seen that although much of the surface is not covered with purple membranes, at the right side the membranes sheets form stacks.

Purple membranes on silanized glass: glass silanized with aminopropyltriethoxysilane has a positive surface charge in water caused by its amino groups. As expected the purple membranes bound to the silanized glass even at neutral pH. In Fig. 3 it can be seen that the surface is uniformly covered with membrane sheets. The image was obtained with 1 mM $CaCl_2$, 10 mM KCl, and 5 mM Tris[hydroxymethyl]aminomethane (Tris), pH 7.2. No overlapping purple membranes were observed. With calcium concentration >5 mM purple membranes began forming stacks.

Purple membrane on lipid bilayers: the function of bacteriorhodopsin was extensively studied on black lipid membranes (24, 25 and references therein). In these experiments a lipid bilayer, called black lipid membrane, separates two compartments filled with electrolyte. The compartments are connected via two electrodes and a current (or voltage) amplifier. When purple membranes are added to one compartment they adsorb to the planar lipid bilayer and after photoexcitation an electric current (or voltage) caused by the proton transport can be seen. In this way the function of purple membranes as a proton pump was studied.

With the AFM purple membranes adsorbed to a lipid bilayer could be visualized (Fig. 4). In distilled water only ~10% of the bilayer was covered with purple membranes. No overlapping purple membranes were observed. Images like Fig. 4 can now be compared to results of functional experiments.

The apparent thickness of the purple membranes depended on the substrate it was adsorbed to. On mica the apparent average thickness was 8.9 ± 2.0 nm, on silanized glass it was 11.1 ± 3.4 nm, and on the lipid bilayer it was 5.2 ± 0.4 nm. These differences are probably due to different interactions between substrate and stylus. However, this discrepancy is not fully understood and needs further investigation. The interactions lipid bilayer/stylus

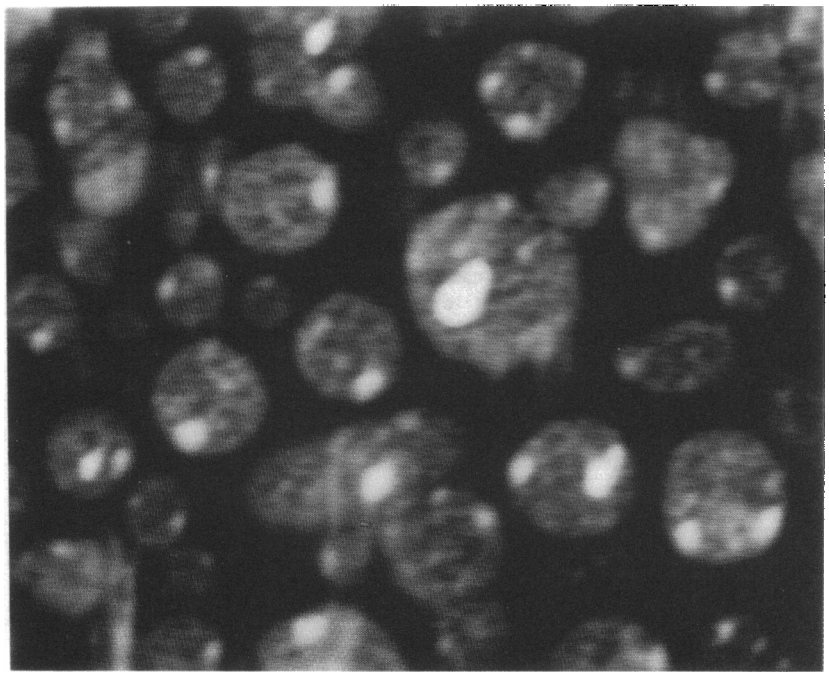

FIGURE 3 Purple membranes adsorbed to glass silanized with aminopropyltriethoxysilane. They were imaged in 1 mM $CaCl_2$, 10 mM KCl, 5 mM Tris, pH 7.2 with a type B cantilever. The image size is 3.8 × 3.5 μm.

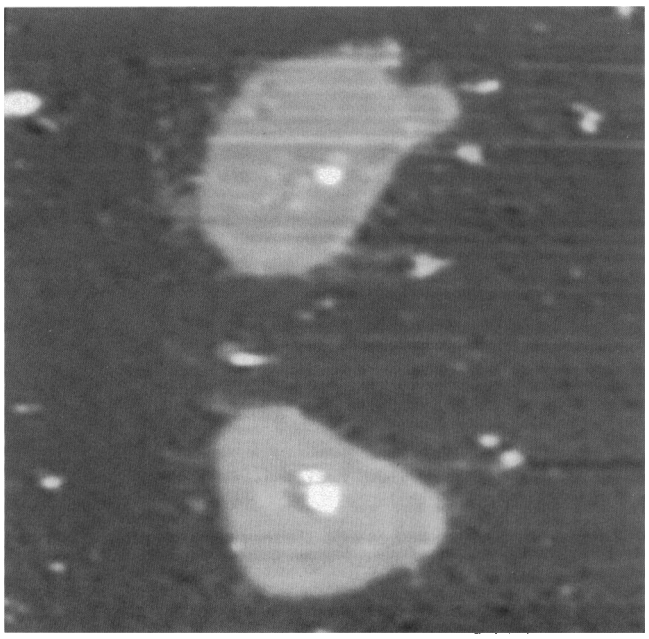

FIGURE 4 Purple membrane bound to a lipid bilayer in distilled water. The image size is 3.3 × 3.3 μm. Cantilever type B.

and purple membrane/stylus are probably similar, so measurements on lipid bilayers should give the best estimates of the real thickness. A purple membrane thickness of 5.2 nm comes close to a value of 4.6 nm, reported by Fisher et al. (33), which is based on scanning tunneling microscope images of metal coated purple membranes.

Molecular resolution of bacteriorhodopsin

To get molecular resolution images of bacteriorhodopsin, we adsorbed purple membranes to mica. When zooming in on regions not covered by purple membranes we observed the hexagonal lattice of mica. As the lattice constant of mica is known to be 0.519 nm (34), the scanner could be calibrated with mica images.

One AFM image obtained on a purple membrane is shown in Fig. 5 *a*. The average value and gradient have been removed from each scan line to reduce the dynamic range. The hexgonal lattice was visible, although the signal-to-noise ratio was rather low. The Fourier transform of this image is shown in Fig. 5 *b*. In 6 of 11 experiments the hexagonal structure could be observed. We measured a lattice constant of 6.21 ± 0.20 nm. Diffraction spots out of the fifth order, corresponding

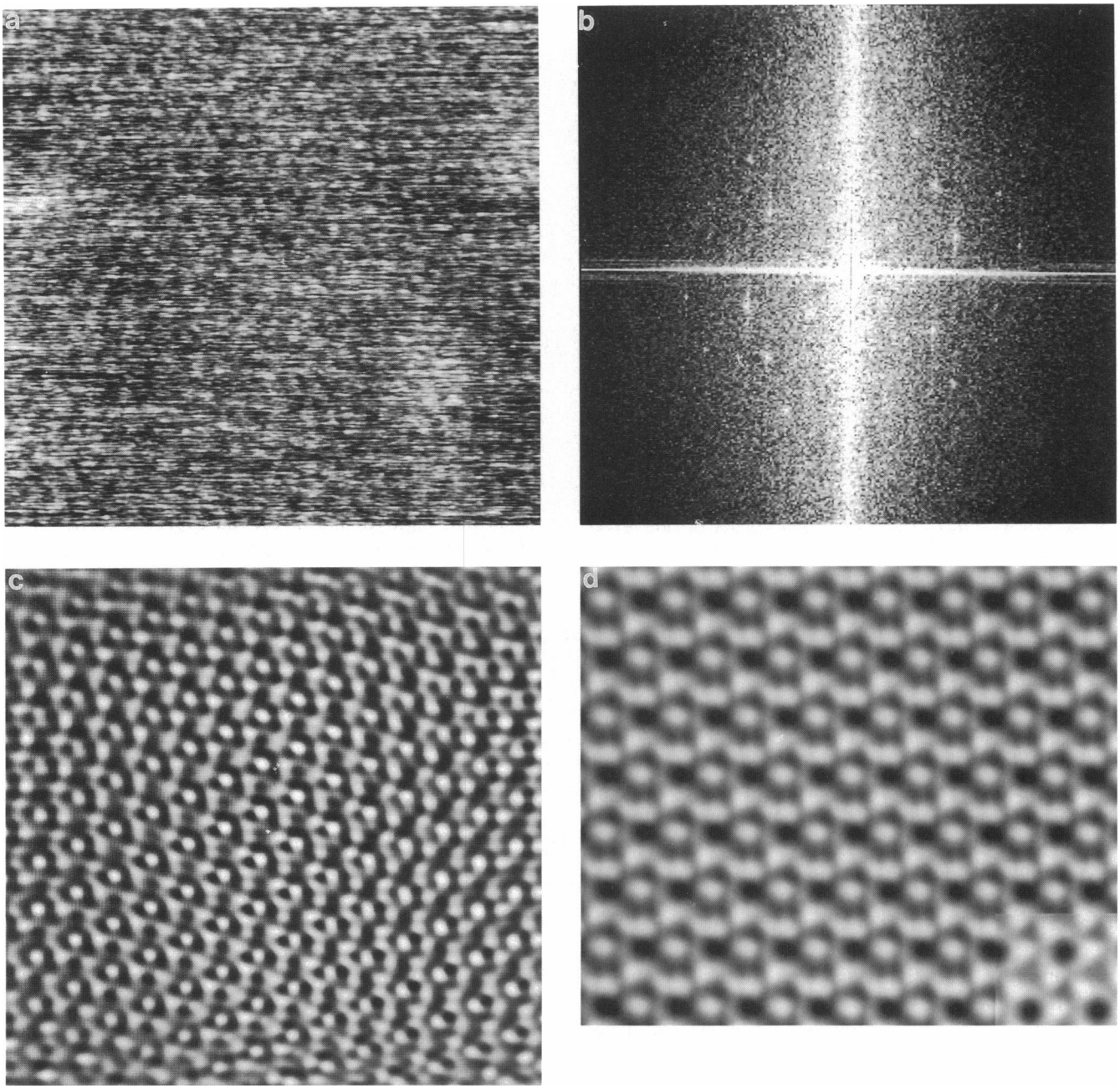

FIGURE 5 (*a*) Image obtained on a purple membrane adsorbed to mica. It was imaged in 2 mM $CaCl_2$, 50 mM NaCl, 10 mM KH_2PO_4, pH 6.5 with a type A cantilever. Light parts are high, dark parts are low. The image size is 79 × 76 nm. *b* shows the two-dimensional Fourier transform of *a*. *c* is a strongly filtered version of *a*. *d* was obtained after unit cell averaging. In the lower right corner the threefold symmetry had been imposed. The image size is 51 × 43 nm.

to a resolution of ~1.1 nm, were often detectable. There was an asymmetry in the pattern, with best resolution and contrast in directions related to the scan direction. This might be due to two reasons. Loosely bound surface structures, for instance the carboxyl terminus, might be pushed by the stylus aligning themself in the scanning direction. In addition, the deformation of the specimen by the stylus might contribute. This deformation, however, was elastic, i.e., the sample was not destroyed as the same area on a purple membrane could be scanned at least

three times without losing surface details. The force had to be kept below ~ 1 nN. When the force was increased above this value, the purple membranes were destroyed, i.e., surface details vanished or even a hole was cut into the membrane.

Fig. 5 *c* is a filtered version of Fig. 5 *a*. It was obtained by masking spots which belonged to the hexagonal structure in the transform (Fig. 5 *b*) with a 6 × 6 pixel box and inverse transforming the masked Fourier transform. With this reduction in the nonperiodic component, the lattice was much more clearly visible, but it is also apparent that there were significant variations in the image across the field. These variations are mainly attributable to the low signal-to-noise ratio of the original image.

To improve the signal-to-noise ratio, we combined and averaged data from three images of the same purple membrane to produce a unit cell image. The data merge with phase errors of ~40 degrees, indicating a fair agreement among the images. The averaged structure is shown in Fig. 5 *d*. In the lower right corner of this image the threefold symmetry of the membrane had been imposed. The symmetrized image should be interpreted cautiously in the light of the tip-induced specimen distortion and asymmetry. Nevertheless it helps to compare our results with results obtained by electron microscopy. In each unit cell three similar bumps arranged in trimers stick out from the surface. Three differently sized deepenings can be distinguished. As the bacteriorhodopsin molecules should look alike, the bumps are interpreted as bacteriorhodopsin molecules. The depressions were identified with the lipid regions as diffraction experiments show three differently sized lipid regions.

We would like to point out that in contrast to diffraction techniques, which require many molecules arranged in a crystal, the AFM images single molecules. The Fourier transform was only used to identify bacteriorhodopsin, to filter the image, and to find the limit of resolution.

A comparison between surface structures of dried purple membrane and purple membrane in buffer is rather difficult as not much is known about the surface structure. AFM images of dried purple membranes (9, 21) show rows with a certain spacing (8.7 nm and 4.9–5.0 nm, respectively). No further details have been resolved in the dried specimen. This is probably due to the high forces of $\sim 10^{-7}$–10^{-8} N applied to the sample when imaging in air (22).

Information obtained by diffraction techniques about the surface structure is rather limited (35). From electron microscope studies of dried purple membranes shadowed with metal or carbon Müller et al. postulated a depression in the region of each bacteriorhodopsin molecule (36). In contrast, Jaffe and Glaeser predicted a depression in the lipid regions of the purple membrane based on electron micrographs obtained from glucose-embedded and frozen hydrated purple membranes (35). Our results obtained in the native environment show a depression in the lipid regions whereas the bacteriorhodopsin molecules are raised. However, it should be kept in mind that the stylus compresses the purple membrane. If the lipids are much softer than the protein, they might appear as depressions even if they have the same height in the incompressed state.

Molecular resolution could not be obtained reproducibly on silanized glass. This is probably due to two reasons. First, the underlying silanized glass is rougher than the atomically flat mica and the surface structure is dominated by the roughness of the silanized glass. Second, the layer of aminopropyltriethoxsilane is a deformable substrate for the membranes sheets. While scanning, the stylus may press the purple membrane down and, thus, increase the contact area between the membrane and the stylus. As the contact area determines the resolution, high resolution can be expected to be more difficult to achieve on deformable substrates. We also did not obtain molecular resolution with the lipid bilayer preparation. Further, we used 200 μm cantilevers for experiments with the fragile lipid bilayer as they apply a lower force to the sample; these have lower sensitivity making it still more difficult to detect single bacteriorhodopsin molecules.

Binding of cationized ferritin to purple membranes

Ferritin, responsible for iron storage, is a ball shaped protein with a diameter of ~12 nm (37). When the carboxyl groups of the protein are coupled with dimethylpropanediamine, the protein becomes positively charged (38). Fisher et al. (38) showed that cationic ferritin binds electrostatically to both sides of the purple membrane.

To image the binding of cationic ferritin to purple membranes, we adsorbed purple membranes to silanized glass as described above. We chose this preparation because purple membranes are tightly bound to the silanized glass whereas cationic ferritin should be repelled electrostatically by the amino groups. In our experiments cationic ferritin was added in a flow-through experiment. Two minutes after adding the cationic ferritin, we could observe the molecules on the uniformly covered purple membranes (Fig. 6). They were identified by several criteria. The balls seen in Fig. 6 were five times bigger than the noise observed when the stylus was not scanning. They could not be observed before adding the cationic ferritin. They could not be seen on areas not covered by purple membranes. They could be scanned several times, and at each scan they appeared at the same place. To obtain Fig. 6 an up and down scan were averaged. The

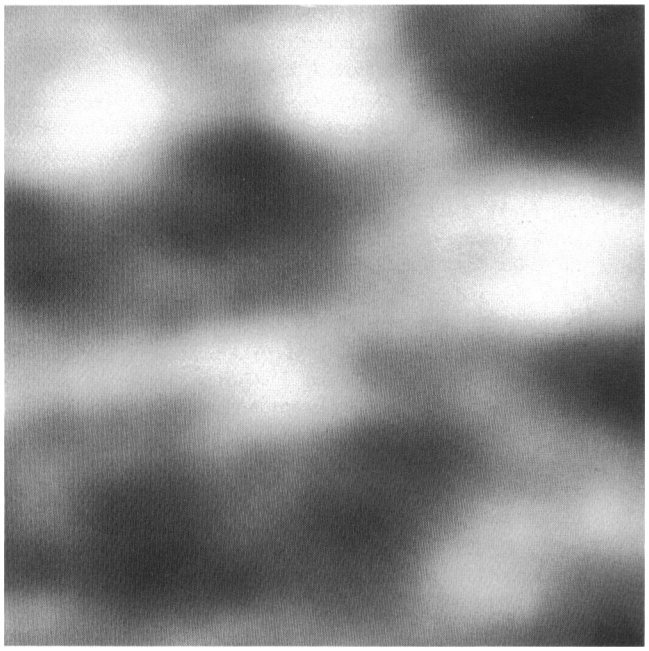

FIGURE 6 Cationized ferritin bound to purple membranes on silanized glass. The image was obtained by averaging the up and down scan of the same area. The image size is 48 × 48 nm. 2 mM $CaCl_2$, 5 mM Tris, pH 7.2, cantilever C.

size of the balls agrees with a value of 12 nm given in the literature for ferritin (37). This image of the binding of cationized ferritin to purple membranes demonstrates the possibility of imaging the binding of a ligand to its receptor with the AFM. Especially exciting is the possibility of imaging binding processes in real time.

CONCLUSION

With the AFM we resolved the surface topography of bacteriorhodopsin down to a resolution of ~1.1 nm. This resolution was obtained in buffer solution, at room temperature and without destroying the sample. Single molecules could be imaged. Depressions were observed in the lipid regions of the purple membrane.

In addition, cationic ferritin bound to purple membrane was imaged. This demonstrates the possibility of studying the binding of ligands to receptors or the binding of antibodies to membrane molecules under native conditions.

Purple membranes adsorbed to a lipid bilayer could also be imaged. These images might help to interpret results of functional studies where puple membranes are bound to black lipid membranes (24, 25).

We thank T. R. Albrecht and C. F. Quate at Stanford University for providing us with microfabricated cantilevers; W. Stoeckenius at University of California San Francisco for providing us with purple membranes and for good advice; H. G. Hansma and H. Gaub for helping us to prepare the lipid bilayers.

This project was supported by National Science Foundation Solid State Physics Grant DMR89-17164 (P. K. H.), the Office of Naval Research (P. K. H.), National Institutes of Health grant GM36884 (K. H. D.), and the Deutsche Forschungsgemeinschaft scholarship Bu 701/1-1 (H.-J. B.).

Received for publication 9 April 1990 and in final form 16 July 1990.

REFERENCES

1. Binnig, G., C. F., Quate, and Ch. Gerber. 1986. Atomic force microscope. *Phys. Rev. Lett.* 56:930–933.
2. Wickramasinghe, H. K. 1989. Scanned-probe microscopes. *Sci. Am.* 260:98–105.
3. Binnig, G., Ch. Gerber, E. Stoll, T. R. Albrecht, and C. F. Quate. 1987. Atomic resolution with atomic force microscope. *Europhys. Lett.* 3:1281–1286.
4. Albrecht, T. R., and C. F. Quate. 1987. Atomic resolution imaging of a nonconductor by atomic force microscopy. *J. Appl. Phys.* 62:2599–2602.
5. Gould, S. A. C., O. Marti, B. Drake, L. Hellemans, C. E. Bracker, P. K. Hansma, N. L. Keder, M. M. Eddy, and G. D. Stucky. 1988. Molecular resolution images of amino acid crystals with the atomic force microscope. *Nature* (*Lond.*). 332:332–334.
6. Drake, B., C. B. Prater, A. L. Weisenhorn, S. A. C. Gould, T. R. Albrecht, C. F. Quate, D. S. Cannell, H. G. Hansma, and P. K. Hansma. 1989. Imaging crystals, polymers, and processes in water with the atomic force microscope. *Science* (*Wash. DC*). 243:1586–1589.
7. Weisenhorn, A. L., M. Egger, F. Ohnesorge, S. A. C. Gould, S.-P. Heyn, H. G. Hansma, R. L. Sinsheimer, H. E. Gaub, and P. K. Hansma. 1990. Molecular-resolution images of Langmuir-Blodgett films and DNA by atomic force microscopy. *Langmuir.* In press.
8. Marti, O., H. O. Ribi, B. Drake, T. R. Albrecht, C. F. Quate, and P. K. Hansma. 1988. Atomic force microscopy of an organic monolayer. *Science* (*Wash. DC*). 239:50–52.
9. Gould, S. A. C., B. Drake, C. B. Prater, A. L. Weisenhorn, S. Manne, H. G. Hansma, P. K. Hansma, J. Massie, M. Longmire, V. Elings, B. Dixon Northern, B. Mukergee, C. M. Peterson, W. Stoeckenius, T. R. Albrecht, and C. F. Quate. 1990. From atoms to integrated circuit chips, blood cells, and bacteria with the atomic force microscope. *J. Vac. Sci. Technol. A.* 8:369–373.
10. Blaurock, A. E., and W. Stoeckenius. 1971. Structure of the purple membrane. *Nat. New Biol.* 233:152–155.
11. Henderson, R. 1975. The structure of the purple membrane from *Halobacterium halobium:* analysis of the x-ray diffraction pattern. *J. Mol. Biol.* 93:123–138.
12. Henderson, R., and P. N. T. Unwin. 1975. Three-dimensional model of purple membrane obtained by electron microscopy. *Nature* (*Lond.*). 257:28–32.
13. Henderson, R., J. M. Baldwin, K. H. Downing, J. Lepault, and F. Zemlin. 1986. Structure of purple membrane from *Halobacterium halobium:* recording, measurement, and evaluation of elec-

tron micrographs at 3.5 Å resolution. *Ultramicroscopy.* 19:147–178.

14. Henderson, R., J. M. Baldwin, T. A. Ceska, F. Zemlin, E. Beckmann, and K. H. Downing. 1990. A model for the structure of bacteriorhodopsin based on high resolution electron cryo-microscopy. *J. Mol. Biol.* 213:899–929.
15. Seiff, F., J. Westerhausen, I. Wallat, and M. P. Heyn. 1986. Location of the cyclohexene ring of the chromophore of bacteriorhodopsin by neutron diffraction with selectively deuterated retinal. *Proc. Natl. Acad. Sci. USA.* 83:7746–7750.
16. Jubb, J. S., D. L. Worcester, H. L. Crespi, and G. Zaccai. 1984. Retinal location in purple membrane of *Halobacterium halobium:* a neutron diffraction study of membranes labelled in vivo with deuterated retinal. *EMBO (Eur. Mol. Biol. Organ.) J.* 3:1455–1461.
17. Engelman, D. M., and G. Zaccai. 1980. Bacteriorhodopsin is an inside-out protein. *Proc. Natl. Acad. Sci. USA.* 77:5894–5898.
18. Trewhella, J., S. Anderson, R. Fox, E. Gogol, S. Khan, D. Engelman, and G. Zaccai. 1983. Assignment of segments of the bacteriorhodopsin sequence to positions in the structural map. *Biophys. J.* 42:233–241.
19. Popot, J-L., D. M. Engelman, O. Gurel, and G. Zaccai. 1989. Tertiary structure of bacteriorhodopsin. Positions and orientations of helices A and B in the structural map determined by neutron diffraction. *J. Mol. Biol.* 210:829–847.
20. Worcester, D. L., R. G. Miller, and P. J. Bryant. 1988. Atomic force microscopy of purple membranes. *J. Microsc. (Oxf.).* 152:817–821.
21. Worcester, D. L., H. S. Kim, R. G. Miller, and P. J. Bryant. 1990. Imaging bacteriorhodopsin lattices in purple membranes with atomic force miroscopy. *J. Vac. Sci. Technol.* A8:403–405.
22. Weisenhorn, A. L., P. K. Hansma, T. R. Albrecht, and C. F. Quate. 1989. Forces in atomic force microscopy in air and water. *Appl. Phys. Lett.* 54:2651–2653.
23. Guckenberger, R., W. Wiegräbe, A. Hillebrand, T. Hartmann, Z. Wang, and W. Baumeister. 1989. Scanning tunneling microscopy of hydrated bacterial surface protein. *Ultramicroscopy.* 31:327–332.
24. Bamberg, E., H.-J. Apell, N. A. Dencher, W. Sperling, H. Stieve, and P. Läuger. 1979. Photocurrents generated by bacteriorhodopsin on planar bilayer membranes. *Biophys. Struct. Mech.* 5:277–292.
25. Holz, M., M. Lindau, and M. P. Heyn. 1988. Distributed kinetics of the charge movements in bacteriorhodopsin: Evidence for conformational substates. *Biophys. J.* 53:623–633.
26. Gould, S. A. C., B. Drake, C. B. Prater, A. L. Weisenhorn, S. Manne, G. L. Kelderman, H.-J. Butt, H. G. Hansma, P. K. Hansma, and S. Maganov. 1990. The atomic force microscope: A tool for science and industry. *J. Microsc. (Oxf.).* In press.
27. Amer, N. M., and G. Meyer. 1988. A simple optical method for the remote sensing of stylus deflection in atomic force microscopy. *Bull. Am. Phys. Soc.* 33:319.
28. Meyer, G., and N. M. Amer. 1988. Novel optical approach to atomic force microscopy. *Appl. Phys. Lett.* 53:2400–2402.
29. Alexander, S., L. Hellemans, O. Marti, J. Schneir, V. Elings, P. K. Hansma, M. Longmire, and J. Gurley. 1989. An atomic-resolution atomic force microscope implemented using an optical lever. *Appl. Phys. Lett.* 65:164–167.
30. Oesterhelt, D., and W. Stoeckenius. 1974. Isolation of the cell membrane of *Halobacterium halobium* and its fractionation into red and purple membrane. *Methods Enzymol.* 31:667–678.
31. Leyden, D. E., editor. 1986. Silanes, Surfaces and Interfaces. Gordon and Breach Science Publishers, New York.
32. Heuser, J. 1989. Protocol for 3-D visualization of molecules on mica via the quick-freeze, deep-etch technique. *J. Electron Microsc. Tech.* 13:244–263.
33. Fisher, K. A., S. L. Whitfield, R. E. Thomson, K. C. Yanagimoto, M. G. L. Gustafsson, and J. Clarke. 1990. Measuring changes in membrane thickness by scanning tunneling microscopy. *Biochim. Biophys. Acta.* In press.
34. Güven, N. 1971. The crystal structures of $2M_1$ phengite and $2M_1$ muscovite. *Z. Kristallogr.* 134:196–212.
35. Jaffe, J. S., and R. M. Glaeser. 1987. Difference Fourier analysis of surface features of bacteriorhodopsin using glucose-embedded and frozen-hydrated purple membranes. *Ultramicroscopy.* 23:17–28.
36. Müller, T., H. Gross, H. Winkler, and H. Moor. 1985. High resolution shadowing with pure carbon. *Ultramicroscopy.* 16:340–348.
37. Theil, E. C. 1987. Ferritin: structure, gene regulation, and cellular function in animals, plants, and microorganisms. *Annu. Rev. Biochem.* 56:289–315.
38. Fisher, K. A., K. Yanagimoto, and W. Stoeckenius. 1978. Oriented adsorption of purple membrane to cationic surfaces. *J. Cell Biol.* 77:611–621.